Fabrication of high voltage square pulse generators for electrooptic Kerr relaxation studies

R. Usha and T. A. PrasadaRao

Citation: Review of Scientific Instruments **65**, 3282 (1994); doi: 10.1063/1.1144564
View online: http://dx.doi.org/10.1063/1.1144564
View Table of Contents: http://scitation.aip.org/content/aip/journal/rsi/65/10?ver=pdfcov
Published by the AIP Publishing

Fabrication of high voltage square pulse generators for electro-optic Kerr relaxation studies

R. Usha and T. A. PrasadaRao
Laser Laboratory, Department of Physics, Indian Institute of Technology, Madras-600036, India

(Received 30 March 1994; accepted for publication 5 June 1994)

High voltage square pulse generators, with fall times of 1 μs and 45 ns have been fabricated for the measurement of electro-optic Kerr relaxation studies in macromolecules. These have been fabricated with a pulse forming network in the Blumlein line configuration with discrete components. The switching is brought about by high voltage spark gaps, instead of the thyratrons and silicon controlled rectifiers (SCRs), which have voltage limitations. The performance of these pulse generators are found to be consistent and stable, without any change in the pulse shape even at very high voltages and repetition rates. The Kerr constants and relaxation times measured with these pulse generators for the liquid crystal *p*-(methoxybenzelidene)-*p*-butylaniline (MBBA) at its nematic to isotropic phase transition temperature (43.5 °C) are found to be in very good agreement with the reported values obtained from the optical Kerr effect investigations using high power Q-switched solid state lasers.

I. INTRODUCTION

The electro-optic Kerr effect[1] is a third order nonlinear process produced when very high electric fields are applied to an optically isotropic material. The material becomes anisotropic under the action of the field and hence becomes birefringent. This effect is molecular or dipolar in origin, and is primarily due to the interaction of the applied field with the permanent dipole moment and/or the anisotropy of polarizability of the molecules. The decay of this induced birefringence upon the instantaneous removal of the orienting field gives a measure of the relaxation time. In order to measure this relaxation time a square pulse with a fast decay is applied to the medium to induce birefringence.

The transient Kerr effect is being widely used in the field of macromolecules like colloidal suspensions,[2,3] biomolecules,[4–6] polymers,[7] etc. for the determination of orientation relaxation times, rotational diffusion constants, and molecular structure parameters.

The Kerr constant of some liquid crystals are found to be exceptionally large just above their nematic to isotropic phase transition temperature T_{NI} with slow relaxation times.[8] This is basically due to the pretransitional behavior of the material. The Kerr constant and relaxation time measurements provide a stringent test on the Landau–de Gennes[10] phase transition model for liquid crystals. From these measurements one can obtain a large number of characteristic material parameters like, the fictitious second order isotropic-nematic transition temperature (T^*), the temperature dependent viscosity coefficient (ν), the phenomenological constants in the Landau series expansion of free energy, etc. These are very important parameters for characterizing a liquid crystal molecule. The decay of birefringence is an exponential function of time and is given as

$$\Delta n = \Delta n_0 \exp(-t/\tau). \tag{1}$$

Δn and Δn_0 are the birefringence at any time t and at $t=0$, respectively. τ is the electro-optic Kerr relaxation time. The induced birefringence Δn is a quadratic function of the applied field

$$\Delta n = B\lambda E^2. \tag{2}$$

E is the applied electric field strength, λ is the probe wavelength, B is the electro-optic Kerr constant.

The description of the experimental setup to measure the induced birefringence and the electro-optic Kerr relaxation time is as follows.

II. EXPERIMENTAL SETUP

Figure 1 shows the schematic of the experimental setup used to measure B and τ. Optical signals of the order of 1 ns duration could be detected using a photodiode (MRD-510, Motorola) across a load of 50 Ω. The Kerr signals from the Photodiode are acquired by a digital storage oscilloscope (DSO) (Tek 2440) with 350 MHz bandwidth. The signals are then transferred to an AT 386 PC for further analysis. The high voltage square pulses are acquired on the DSO through a 1:1000 high voltage probe (Tektronix P6015) simultaneously along with the Kerr signals. The magnitude of the phase difference produced by the field (E) is

$$\delta/2 = (\pi l/\lambda) \quad \text{and} \quad \Delta n = \pi l B E^2, \tag{3}$$

where l is the effective path length of the probe beam in the electric field. δ can be determined from the experiment using the relation[11]

$$I = I_0 \sin^2(\delta/2), \tag{4}$$

where I_0 is the maximum intensity of the probe beam when the polarizer and the analyzer are kept parallel and I is the maximum intensity of light passing through the medium under the influence of the electric field when the polarizer and the analyzer are kept crossed and making an angle of 45° with respect to the direction of the applied electric field.

The details of the fabrication of the pulse generators and their application in the measurement of Kerr constants and

 0034-6748/94/65(10)/3282/4/$6.00

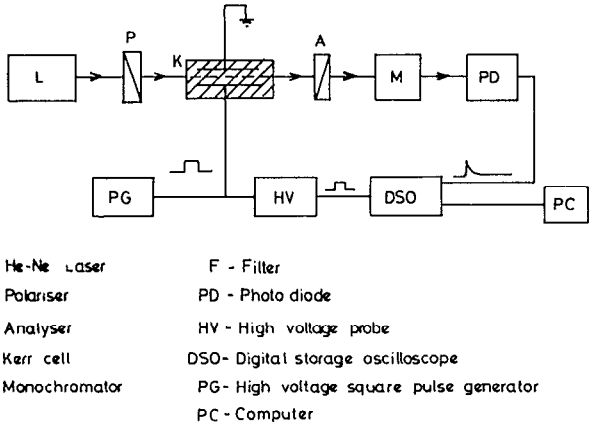

FIG. 1. Experimental setup for Kerr effect studies.

Kerr relaxation times in the liquid crystal *p*-(methoxybenzelidene)-*p*-butylaniline (MBBA) at its phase transition temperature are discussed in the following sections.

III. PRINCIPLE OF OPERATION AND FABRICATION OF THE PULSE GENERATOR

Usually a low impedance delay line which is either continuous or discrete, with thyratrons or silicon controlled rectifiers (SCRs) as high voltage (HV) switches are used for pulse generators in the studies of transient Kerr effect.[12] The discharge of a transmission line or a delay line into its characteristic load produces a square pulse. But the voltage at the load is only half the charging voltage of the capacitors. Figure 2(a) illustrates the circuit of a single transmission line. By using two transmission lines instead of one in a Blumlein configuration as shown in Fig. 2(b), square pulses with voltages equal to the charging voltage of the capacitors could be produced. The Blumlein line configuration also acts as a pulse shaping network. Discrete components like capacitors and inductors are also being used instead of a transmission line shown to produce[13,14] the same results.

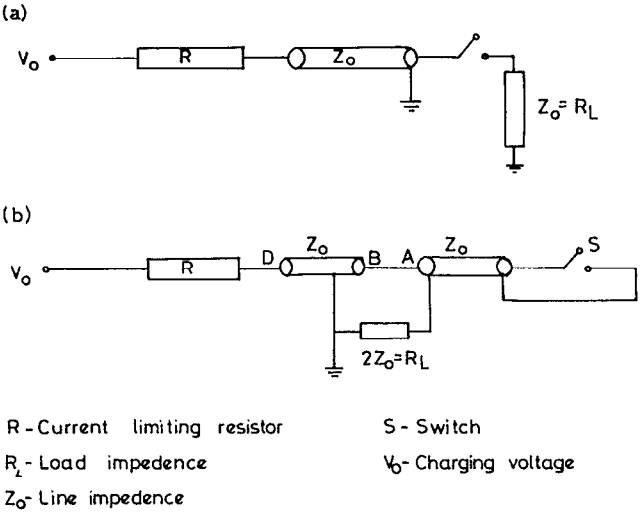

FIG. 2. (a) Typical single transmission line. (b) Two transmission lines in Blumlein configuration.

A. Layout of a Blumlein

The Blumlein network as shown in Fig. 2(b), consists of two line sections of equal length and equal impedance Z_0 with a load resistance $R_l = 2Z_0$. The line is charged up to a voltage V_0. When the switch S is closed, a wave starts at S and travels along SA. After the transmission time t_0, a second wave is excited at B which travels along BD. Both waves are reflected at the inhomogeneities of the line. The potential difference between A and B prduced by these waves appears as a square pulse which has an amplitude V_0 and duration $2t_0$.

B. Theory of a Blumlein

Glasoe and Lebacqz[15] have done extensive theoretical calculations for these pulse forming networks for various pulse shapes. The results of such theoretical analysis for a square pulse produced with a pulse forming network with a Blumlein line configuration are presented below.

The Blumlein line consists of two sections, each of which comprises n symmetrical T elements, with an inductance L in series and a capacitance C in parallel.

The transition time along one section of the line is

$$t_0 = n(LC)^{1/2}. \tag{5}$$

The pulse duration is

$$T = 2t_0 = 2n(LC)^{1/2}. \tag{6}$$

The line impedance Z_0 is

$$Z_0 = (L/C)^{1/2}. \tag{7}$$

The load resistance to be used to get a perfect square pulse is

$$R_1 = 2(Z_0) = 2(L/C)^{1/2}. \tag{8}$$

The pulse rise time τ is

$$\tau = \pi(LC)^{1/2}/4. \tag{9}$$

The inductance and the capacitance are then determined by the relations

$$nC = T/R_1 \quad \text{and} \quad L = TR_1/(4n). \tag{10}$$

For a pulse of a particular rise, fall, and width, the values of n, C, and L are calculated approximately and are used in the circuit.

C. Fabrication

The Blumlein line consisting of L and C in the T configuration is shown in Fig. 3. A load resistance R_1 which matches with the line impedance in order to produce a perfect square pulse, is connected in between the two sections of the line. The Kerr cell is connected across the load R_1. A dc high voltage power supply (0–25 kV) is connected to one section of the line, through a current limiting resistor R (1 MΩ). A high voltage spark gap has been used as a switching element. The pulse voltage is limited only by the power sup-

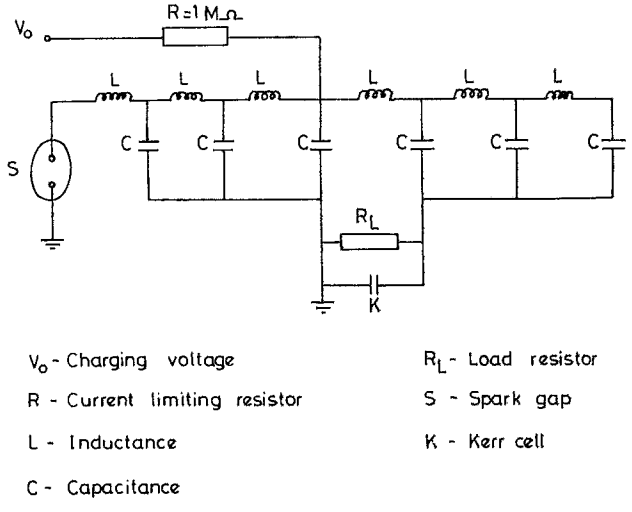

FIG. 3. Discrete transmission line in the Blumlein configuration.

ply used in the circuit but not by the switching element unlike the circuits with thyratrons or SCRs that have high voltage limitations. The capacitors are made of glass epoxy sheets with copper claddings on both sides. The value of the capacitors can be monitored by the area of the sheets. The inductors used are hand wound using an insulated copper wire of 1 mm thickness. These capacitors and inductors can also withstand voltages as high as 40 kV. The spark gap was either self triggered or externally triggered. External triggering was operated with a HV trigger pulse generator which also forms part of the setup.

In the case of a microsecond pulse generator six sets of 1.5 nF capacitors and 65 μH inductors are used in the T configuration in the circuit shown in Fig. 3. Each section of the Blumlein consists of three T elements with a load $R_1=450\ \Omega$ in between. Stable pulses with 1 μs rise and fall and 1.6 μs flattop have been obtained. The same circuit is also used for the nanosecond pulse generator with 16 sets of 70 pF capacitors and 1.5 μH inductors. Each section of the Blumlein consists of eight T elements with a load $R_1=300\ \Omega$ in between. The square pulses obtained are stable with 45 ns rise and fall and 150 ns flattop.

The pulses obtained with the pulse generator and the corresponding Kerr signals are shown in the Fig. 4. It is found that there is a small deviation in the pulse characteristics from the one calculated for a homogeneous transmission line. A slight ringing is also present in the beginning of the pulse. These are due to the losses and the dispersion of the line caused by the lumped structure. The pulse parameters obtained with the pulse generators along with the calculated values using the above relations are given in Table I.

D. Salient features

The two pulse generators fabricated have excellent, reliable, and stable characteristics, like

(1) short fall times,
(2) flattop with minimum ringing,
(3) voltages variable from 0 to 25 kV that are limited by the power supply used in the present work,

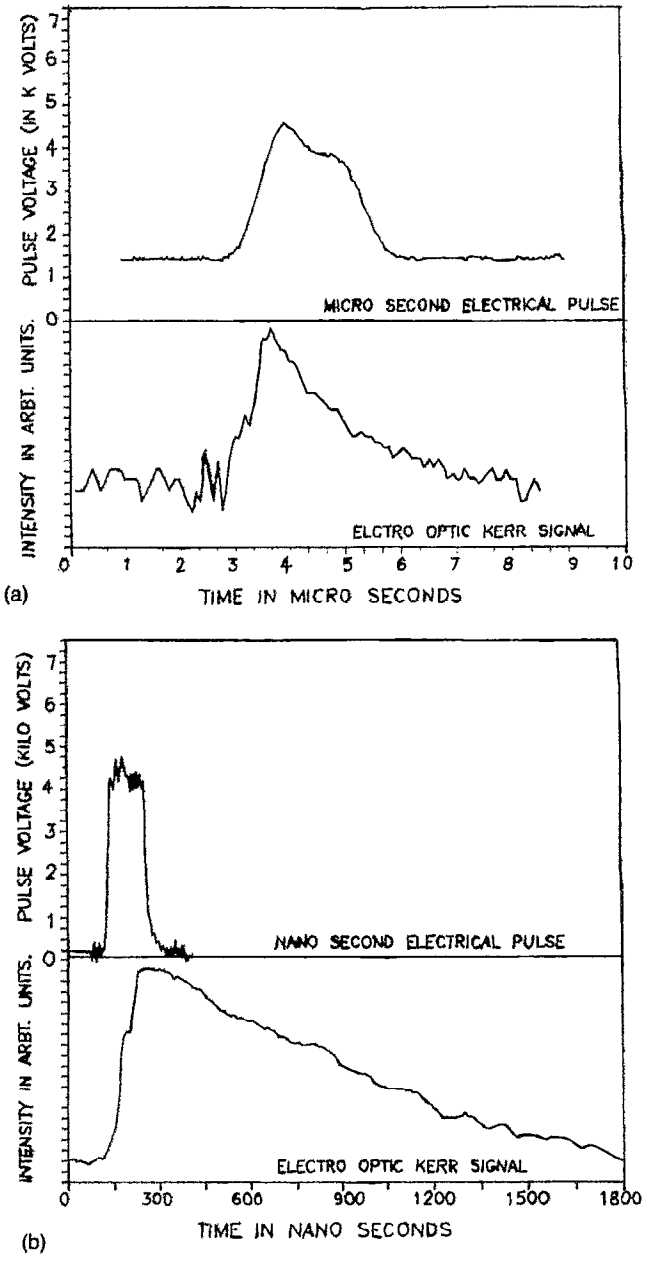

FIG. 4. (a) Kerr signal in MBBA induced by a microsecond pulse. (b) Kerr signal in MBBA induced by a nanosecond pulse.

(4) highly consistent and stable pulses with absolutely no change in pulse shapes even at high voltages and high repetition rates, and
(5) are very cost effective since all the components are fabricated with cheap and easily available materials.

TABLE I. Pulse parameters of the μs and ns pulses.

Pulse generator		Line impedance $Z_0=R_L/2\ \Omega$	Pulse width T μs	Pulse rise time t_a μs
Microsecond	Calculated	208	1.87	0.73
(μs)	Experimental	225	1.6	1.00
Nanosecond	Calculated	146	0.163	0.064
(ns)	Experimental	150	0.15	0.05

TABLE II. Kerr constant (B) and Kerr relaxation times (τ).

Sample	Nitrobenzene $B(10^{-15}$ m/V$^2)$	Benzoylchloride $B(10^{-15}$ m/V$^2)$	MBBA at T_{NI} $B(10^{-15}$ m/V$^2)$	$\tau(10^{-6}$ s)
Experimental	3500	2230	9400	1.05
Reported	3552[a]	2260[a]	9700[a]	>0.8[b]

[a]Reference 16.
[b]Reference 17.

IV. RESULTS

Initially the high voltage square pulses obtained from these two pulse generators are used to estimate the Kerr constants (B) of nitrobenzene and benzoylchloride to standardize the entire electro-optical setup and the results along with the previously reported values[16] are presented in Table II.

The electro-optic Kerr relaxation time and the Kerr constant for a nematic liquid crystal MBBA has been determined at its phase transition temperature (43.5 °C), using both the pulse generators. The relaxation times obtained experimentally, using the nanosecond and the microsecond pulse generators are 1.05 and 0.8 μs, respectively. Earlier the optical Kerr relaxation time for MBBA at its phase transition temperature T_{NI} had been reported[17,8] as greater than 0.8 and 0.5 μs, respectively. Here the authors have used a 10 ns Q-switched ruby laser pulse (λ=6943 Å) and a 50 ns Q-switched Nd-YAG laser pulse (λ=1064 Å), respectively. The electro-optic Kerr relaxation time obtained with our nanosecond pulse generator is found to be closer to the value (>0.8 μs) obtained in the optical Kerr relaxation time measurements reported earlier.[17] Kerr relaxation has also been observed in MBBA with the microsecond pulse generator. But the result obtained with the nanosecond pulse generator is found to be more accurate and reliable since the Kerr relaxation time in MBBA is much greater than the pulse fall time (45 ns) compared to the pulse fall time (1 μs) of the microsecond pulse generator. The values of the Kerr constant and the relaxation time in MBBA are included in Table II.

The liquid samples used for standardization in our studies are of spectroscopic grade and were also distilled well before use. The liquid crystal sample was obtained from Aldrich and has been used without further purification.

The microsecond pulse can be used in the case of macromolecules where the relaxation times are much greater than the electrical pulse fall time. The pulse parameters can be changed, according to the requirement of the sample under investigation, just by varying the number and values of the inductors (L) and capcitors (C) used. Similarly the pulse shape could also be varied as needed by altering the geometry in which L and C are connected.

ACKNOWLEDGMENTS

One of the authors (R. Usha) wishes to thank S. Arathi-Rani for the help extended during the fabrication of the pulse generator.

[1] J. Kerr, Philos. Mag. **50**, 337 (1875).
[2] H. J. Jerrard, C. L. Riddford, and P. Ingram, J. Sci. Instrum. (J. Phys. E) **2**, 761 (1969).
[3] C. L. Riddford and B. R. Jennings, Adv. Mol. Relat. Interface Proc. **10**, 15 (1977).
[4] C. L. Riddford and B. R. Jennings, Biopolymers **5**, 757 (1967).
[5] D. Bourret, J. Mol. Liq. **30**, 85 (1985).
[6] D. Bourret, J. Mol. Liq. **40**, 37 (1989).
[7] K. Weir and B. R. Jennings, J. Sci. Instrum (J. Phys. E) **22**, 1037 (1989).
[8] H. J. Coles and B. R. Jennings, Mol. Phys. **31**, 571 (1976).
[9] I. C. Khoo, *Progress in Optics* (Elsevier Science, New York, 1988), Vol. XXVI.
[10] P. G. De Gennes, Mol. Cryst. Liq. Cryst. **12**, 193 (1971); P. G. De Gennes, Phy. Lett. A **30**, 454 (1969).
[11] H. J. Jerrard, J. Opt. Soc. Am. **38**, 35 (1948).
[12] D. Bourret, and J. Vigo, J. Mol. Liq. **50**, 135 (1991).
[13] K. Gasthaus and A. Stampa, J. Sci. Instrum (J. Phys. E) **20**, 192 (1987).
[14] J. Montanhha, M. Egberto, and B. Villiaverde, Meas. Sci. Tech. **2**, 1026 (1991).
[15] G. N. Glasoe and J. V. Lebacqz, *Pulse Generators*, Radiation Lab Series (McGraw-Hill, New York, 1948).
[16] J. Philip and T. A. PrasadaRao, J. Mol. Liq. **48**, 85 (1991).
[17] G. K. L. Wong and Y. R. Shen, Phys. Rev. Lett. **30**, 895 (1973).
[18] T. W. Stinson and J. D. Lister, Phys. Rev. Lett. **25**, 503 (1970).